Connected Vehicle Data-Aided Ramp Metering for Distant Bottlenecks Induced by Traffic Accidents

Yu Tang[1], Jingqin Gao[2], Fan Zuo[3], Di Sha[1], and Kaan Ozbay*[4,5]

[1]Ph.D. candidate, Department of Civil and Urban Engineering, New York University, U.S.
[2]Assistant Director of Research, C2SMARTER Center, New York University, U.S.
[3]Postdoctoral Research Associate, C2SMARTER Center, New York University, U.S.
[4]Professor, Department of Civil and Urban Engineering, New York University, U.S.
[5]Director, C2SMARTER Center, New York University, U.S.

Short summary

This paper explores the enhancement of ramp metering strategies using data from connected vehicles (CVs), specifically targeting non-recurrent bottlenecks caused by traffic accidents. Traditional ramp metering, which relies on fixed sensors for feedback control, is often ineffective in managing these unpredictable, distant bottlenecks. However, this issue may become more tractable in a CV environment, as CVs can serve as mobile sensors, providing broader spatial coverage and generating more granular speed and position data. In this paper, we proposed using CV data to estimate bottleneck-related traffic states for implementing feed-forward ramp metering algorithms that addresses congestion around distant bottlenecks. Our method was tested and validated in a micro-simulation model, across various CV scenarios, with different market penetration scenarios. The findings indicate improved traffic mobility and more effective responses to accident-induced bottlenecks in a CV-enhanced ramp metering system both at the local and system level.
Keywords: Connected vehicles, Traffic management, Ramp metering, Traffic simulation

1 Introduction

The recent advances in connected vehicles (CVs) have enabled the generation and sharing of more fine-grained data, such as Basic Safety Messages (BSMs) (Vasudevan et al., 2022). This development presents an opportunity to enhance traffic management strategies aimed at improving traffic flow and safety. The access to granular vehicle-level data enables more accurate estimations of traffic states, even in mixed traffic consisting of CVs and non-CVs (Wang et al., 2022). Consequently, this leads to a refinement of control implementations.

A review of the existing literature reveals that main limitations identified in the existing ramp metering control include inaccuracies in vehicle position leading to unreliable queue estimations, and inadequate detection coverage by fixed infrastructure (e.g, loop detectors), resulting in a lack of accurate situational awareness of changing road conditions (Vasudevan et al., 2024)]. To address these limitations, current research in ramp metering with CV data has employed various approaches. For instance, some studies have applied deep reinforcement learning that directly handles high-dimensional inputs to implement ramp metering (Hou et al., 2021). Others have investigated coordinated control among multiple on-ramps (Zhao et al., 2019; Heshami & Kattan, 2021), or together with other control strategies such as vehicle lane changing (Tajdari et al., 2020).

However, it is important to note that these studies primarily focus on using CV data-aided ramp metering for recurrent congestion or bottlenecks near ramps. The challenge increases significantly when dealing with a distant bottleneck located far downstream from the ramp. In such case, when metered traffic reaches the distant downstream bottleneck, the state of the bottleneck may have significantly changed from the time it was initially assessed for computing the metering rate (Zhou et al., 2020). The lengthy travel time between the ramp and the bottleneck introduces time-delay effects, which poses substantial stability challenges. This raises the need for more dynamic and informative ramp metering strategies that can effectively handle such complex traffic scenarios.

This study introduces a new approach in enhancing both local and system-wide ramp metering algorithms using BSM data from CVs, particularly targeting freeway operations affected by distant bottlenecks (e.g., by traffic accidents). The innovative aspect of this research lies in integrating feed-forward control into feedback ramp metering, coupled with the design of the control algorithm that incorporates more precise traffic information from CV data, including flow, travel time, and density, around incidents to manage distant bottlenecks effectively. Traditionally, such information from a distant bottleneck is often "unknown" or inaccurate given traditional sensors. Consequently, this paper demonstrates how to develop an improved freeway operation strategy that leverages the advantages of CV data as supplemental input into the ramp metering algorithms.

2 Methodology

This section first introduces state-of-the-practice local and system-wide ramp metering. Then we present the methods of using CV data to estimate traffic states related to distant bottlenecks. It is followed by enhancement of the ramp metering algorithms given those estimations.

State-of-the-practice ramp metering algorithms

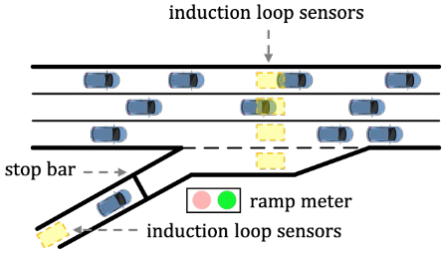

Figure 1: Practical sensor layout required by ALINEA.

We start from locally responsive ramp metering, for which ALINEA is one of the most widely-used algorithms (Papageorgiou et al., 1991). ALINEA exploits the occupancy measured by induction loops, typically downstream of the on-ramp (Figure 1). For on-ramp i, the metering rate (vehicles per hour) at time step t as per the ALINEA algorithm, denoted by $r_i^{\mathsf{loc}}(t)$, is given by

$$r_i^{\mathsf{loc}}(t+1) = r_i^{\mathsf{loc}}(t) + K_i(\hat{o}_i^{\mathsf{main}} \quad o_i^{\mathsf{main}}(t)) \tag{1a}$$

$$r_i^{\mathsf{loc}}(t+1) = \max\{\min\{r_i^{\mathsf{loc}}(t+1), R_i^{\mathsf{max}}\}, R_i^{\mathsf{min}}\}, \tag{1b}$$

where K_i is the control gain, $o_i^{\mathsf{main}}(t)$ is the measured mainline occupancy, $\hat{o}_i^{\mathsf{main}}$ is the corresponding critical occupancy, namely the optimal occupancy, R_i^{max} and R_i^{min} are the maximum and minimum metering rates, respectively. Clearly, equation (1a) indicates that higher occupancy measurements lead to lower metering rates. Equation (1b) shows that the metering rate is bounded by the maximum and minimum metering rates to avoid the well-known wind-up effect (Papamichail & Papageorgiou, 2008).

In practice, to avoid the spillover of on-ramp queues into surrounding urban streets, queue override strategy can be added to the ALINEA algorithm (Smaragdis & Papageorgiou, 2003). This strategy takes into account the occupancy measured at the on-ramp entry, as depicted in Figure 1. Formally, for on-ramp i, the queue override strategy is given by:

$$r_i^{\mathsf{qo}}(t) = \begin{cases} R_i^{\mathsf{min}} & \text{if } o_i^{\mathsf{ramp}}(t) \quad \bar{o}_i^{\mathsf{ramp}}, \\ R_i^{\mathsf{max}} & \text{if } o_i^{\mathsf{ramp}}(t) > \bar{o}_i^{\mathsf{ramp}}, \end{cases} \tag{2}$$

where $\bar{o}_i^{\mathsf{ramp}}$ is the occupancy threshold, and $o_i^{\mathsf{ramp}}(t)$ is the occupancy measured at the on-ramp entry. Finally, for on-ramp i, the metering rate $\tilde{r}_i^{\mathsf{loc}}(t)$ is designed by

$$\tilde{r}_i^{\mathsf{loc}}(t) = \max\{r_i^{\mathsf{loc}}(t), r_i^{\mathsf{qo}}(t)\}. \tag{3}$$

The control law above implies that the metering rate from ALINEA will be overridden if there are too many queueing vehicles at the on-ramp.

Next, we present the system-wide ramp metering, Heuristic Coordinated Ramp Metering (HERO), whose control efficacy has been verified in the field test (Papamichail et al., 2010). HERO utilizes localized ramp metering, such as ALINEA, for individual on-ramps when coordination is not requested; but also includes a heuristic coordination mechanism to coordinate consecutive on-ramps; see Figure 2. Details about the coordination rule are available in Papamichail et al. (2010).

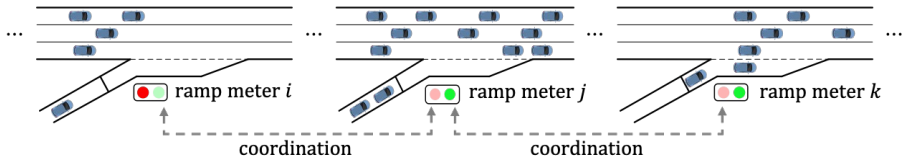

Figure 2: HERO coordinating consecutive on-ramps.

Once on-ramps i and j are coordinated, with on-ramp i as the subordinate and on-ramp j as the master, HERO computes the minimum queue length to be maintained at on-ramp i, $w_i^{\min}(t)$, and the coordinated metering rate for on-ramp i, denoted by $r_i^{\text{co}}(t)$, as follows:

$$w_i^{\min}(t) = \frac{w_i(t) + w_j(t)}{w_i^{\max} + w_j^{\max}} w_i^{\max}, \tag{4a}$$

$$r_i^{\text{co}}(t) = \frac{1}{T}(w_i^{\min}(t) \quad w_i(t)) + q_i^{\text{in}}(t \quad 1), \tag{4b}$$

$$r_i^{\text{co}}(t) = \max\{\min\{r_i^{\text{co}}(t), R_i^{\max}\}, R_i^{\min}\}, \tag{4c}$$

where $w_i(t)$ (resp. $w_j(t)$) denotes the queue length at on-ramp i (resp. j), $w_i^{\max}(t)$ (resp. $w_j^{\max}$) denotes the maximum queue length allowed at on-ramp i (resp. j), T is the control period and $q_i^{\text{in}}(t \quad 1)$ is the flow measurement at the on-ramp entrance at time step $t \quad 1$. The equations (4a)-(4b) above indicate that when on-ramp j has a relatively long queue and high downstream occupancy, HERO attempts to maintain a queue with the length of $w_i^{\min}(t)$ at on-ramp i by enforcing the metering rate $r_i^{\text{co}}(t)$. Besides, the equations (4a)-(4b) imply ramp queue length needs to be estimated from induction loops. Details of the estimation method are available in Papamichail et al. (2010). HERO also introduces queue control to avoid too many vehicles accumulating at on-ramps, namely

$$r_i^{\text{qc}}(t) = \frac{1}{T}(w_i^{\max} \quad w_i(t)) + q_i^{\text{in}}(t \quad 1), \tag{5a}$$

$$r_i^{\text{qc}}(t) = \max\{\min\{r_i^{\text{qc}}(t), R_i^{\max}\}, R_i^{\min}\}. \tag{5b}$$

For on-ramp i, the final metering rate is specified as follows:

$$\tilde{r}_i^{\text{coor}}(t) = \begin{cases} \max\{\min\{r_i^{\text{loc}}, r_i^{\text{co}}(t)\}, r_i^{\text{qc}}(t), r_i^{\text{qo}}(t)\} & \text{if } i \text{ is coordinated,} \\ \max\{r_i^{\text{loc}}(t), r_i^{\text{qc}}(t), r_i^{\text{qo}}(t)\} & \text{if } i \text{ is not coordinated.} \end{cases} \tag{6}$$

Bottleneck information extracted from CV data

The following introduces how to extract bottleneck information from CV data, which is a prerequisite for enhancing the aforementioned ramp metering algorithms for distant bottlenecks. We consider i) vehicle flow entering and exiting the distant bottleneck, ii) travel time from the on-ramp to the bottleneck, and iii) traffic density around the bottleneck; see Figure 3. This paper primarily concentrates on improving ramp metering after traffic accidents happen or are detected. We first use CV data to estimate the traffic flows entering the bottleneck. Those leaving the bottleneck can be estimated in a similar way. Consider a bottleneck illustrated in Figure 3. We denote the tail boundary as follows:

$$S^{\text{tail}}(x, y) = (x_2^{\text{t}} \quad x_1^{\text{t}})(y \quad y_1^{\text{t}}) \quad (y_2^{\text{t}} \quad y_1^{\text{t}})(x \quad x_1^{\text{t}}). \tag{7}$$

Therefore, we have $S^{\text{tail}}(x, y) < 0$ for any downstream position (x, y) and $S^{\text{tail}}(x, y) > 0$ for any upstream position (x, y). This helps determine vehicle locations relative to the bottleneck tail.

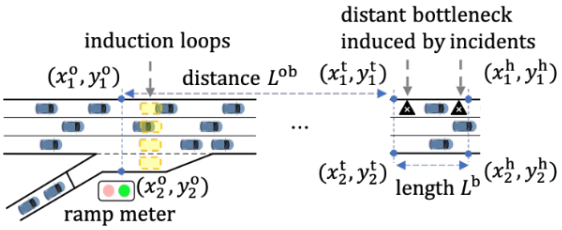

Figure 3: Layout of a distant bottleneck, induced by accidents, downstream of an on-ramp.

Given a set of the CV data collected in a period Δ with N vehicle identifiers, we analyze if there exist two consecutive data points such that one is recorded upstream of the bottleneck tail and the other one downstream of the bottleneck tail, for vehicle $n = 1, 2, \quad , N$. If these data points are identified, we recognize the vehicle passed the boundary during the observation period. Letting N^{tail} denote the total number of vehicles having passed the tail boundary in the period Δ, we obtain the measured flow as follows

$$\tilde{q}^{\mathsf{in}} = N^{\mathsf{tail}}/\Delta. \tag{8}$$

Clearly, due to limitation of CV market penetration rates, potential communication errors and equipment failures, the measured flow $\tilde{q}^{\mathsf{in}}$ can be biased. To address this issue, we utilized induction loop data as a calibration method to reduce the bias. Consider a road section that is already equipped with existing induction loops, e.g., near the on-ramp. From induction loops, we can acquire flow measurements $q_1, q_2, \quad , q_M$ at time steps $1, 2, \quad , M$, to be used as an approximation of the ground truth. At the same time, we apply the estimator (8) to obtain $\tilde{q}_1, \tilde{q}_2, \quad , \tilde{q}_M$ to compute a calibration ratio γ^{ow} as follows:

$$\gamma^{\mathsf{ow}} = \frac{1}{M} \sum_{m=1}^{M} \tilde{q}_m / q_m. \tag{9}$$

Using this calibration ratio, we are able to estimate the flow into the bottleneck by rescaling $\tilde{q}^{\mathsf{in}}$:

$$q^{\mathsf{in}} = \tilde{q}^{\mathsf{in}} / \gamma^{\mathsf{ow}}. \tag{10}$$

For estimating the travel time, let a closed set X^{ob} denote the road segment fron the on-ramp to the bottleneck tail, e.g. the region bounded by the points (x_1^o, y_1^o), (x_2^o, y_2^o), (x_1^t, y_1^t) and (x_2^t, y_2^t) in Figure 3. Assume that the collected CV data has I_n records for vehicle $n = 1, 2, \quad , N$. The travel time from the on-ramp to the bottom tail is estimated by

$$\tau^{\mathsf{ob}} = L^{\mathsf{ob}} \frac{\sum_{n=1}^{N} \sum_{i=1}^{I_n} \mathbb{I}_{X^{\mathsf{ob}}}((x_{n,i}, y_{n,i}))}{\sum_{n=1}^{N} \sum_{i=1}^{I_n} v_{n,i} \mathbb{I}_{X^{\mathsf{ob}}}((x_{n,i}, y_{n,i}))}, \tag{11}$$

where L^{ob} is the distance from the on-ramp to the bottleneck tail, $v_{n,i}$ denotes the speed of vehicle n by the i-th record, $(x_{n,i}, y_{n,i})$ represents the location of vehicle n by the i-th record, and the indicator function implies whether vehicle n generates the i-th record in the region X^{ob}, namely

$$\mathbb{I}_{X^{\mathsf{ob}}}((x_{n,i}, y_{n,i})) = \begin{cases} 1 & \text{vehicle } n \text{ locates in } X^{\mathsf{ob}} \text{ at step } i, \\ 0 & \text{vehicle } n \text{ does not locate in } X^{\mathsf{ob}} \text{ at step } i. \end{cases} \tag{12}$$

Finally, the following illustrates the estimation of traffic density around the bottleneck. Let a closed set X^{b} denote the bottleneck region, e.g. the road segment bounded by the points (x_1^t, y_1^t), (x_2^t, y_2^t), (x_1^h, y_1^h) and (x_2^h, y_2^h) in Figure 3. We can obtain the CV density as follows:

$$\tilde{\rho}^{\mathsf{b}} = \frac{1}{L^{\mathsf{b}} \Delta} \sum_{n=1}^{N} \sum_{i=1}^{I_n} \mathbb{I}_{X^{\mathsf{b}}}((x_{n,i}, y_{n,i})), \tag{13}$$

where L^{b} denotes the bottleneck length, and Δ is the observation period of the CV data. Clearly, $\hat{\rho}^{\mathsf{b}}$ is a biased estimation of real traffic density due to the limitation of CV market penetration rates, communication errors and equipment failures. Similarly, as calibrating $\tilde{q}^{\mathsf{in}}$ given by (8), we

can correct it using the calibration ratio approach:

$$\gamma^{\mathsf{den}} = \frac{1}{M} \sum_{m=1}^{M} \tilde{\rho}_m^{\mathsf{b}} / \rho_m^{\mathsf{b}}, \tag{14a}$$

$$\rho^{\mathsf{b}} = \tilde{\rho}^{\mathsf{b}} / \gamma^{\mathsf{den}}, \tag{14b}$$

where γ^{den} is a rescaling factor that quantifies the differences between the densities of real traffic and the CV data at the bottleneck. Note that the ground truths of traffic densities can be estimated from induction loops or measured by camera sensors.

Enhanced ramp metering algorithms

Our enhanced algorithms are inspired by the feed-forward ALINEA (FF-ALINEA) that was proposed to resolve nearby and distant bottlenecks (Frejo & De Schutter, 2018). It is important to note that FF-ALINEA still relies on induction loops, and in this paper, we present the CV data-aided ramp metering algorithms. We first consider locally responsive ramp metering. Suppose there is a distant bottleneck downstream of on-ramp i. The metering rate for the bottleneck is given by

$$r_i\,(t+1) = r_i\,(t) + K_i\,(\hat{\rho}_i^{\mathsf{b}} \quad \max\{\tau_i^{\mathsf{ob}}(t)(q_i^{\mathsf{b,in}}(t) \quad q_i^{\mathsf{b,out}}(t)), 0\} \quad \rho_i^{\mathsf{b}}(t)), \tag{15a}$$

$$r_i\,(t+1) = \max\{\min\{r_i\,(t+1), R_i^{\mathsf{max}}\}, R_i^{\mathsf{min}}\}, \tag{15b}$$

where $r_i\,(t)$ denotes the metering rate, K_i is the control gain, $\hat{\rho}_i^{\mathsf{b}}$ denotes the critical density around the bottleneck, the travel time $\tau_i^{\mathsf{ob}}(t)$ is given by the estimator (11), flows into and out of the bottleneck are given by the estimator (10), and the density is given by the estimator (14b). Note that (15a) indicates that the density setpoint around the bottleneck is time-varying, i.e.,

$$\hat{\rho}_i^{\mathsf{b}} \quad \max\{\tau_i^{\mathsf{ob}}(t)(q_i^{\mathsf{b,in}}(t) \quad q_i^{\mathsf{b,out}}(t)), 0\} \tag{16}$$

More explanations about the density setpoint can be found in Frejo & De Schutter (2018). The final metering rate can be calculated as follows:

$$\tilde{r}_i^{\mathsf{loc}}\,(t) = \max\{\min\{r_i^{\mathsf{loc}}(t), r_i\,(t)\}, r_i^{\mathsf{qo}}(t)\} \tag{17}$$

Clearly, the enhanced system-wide ramp metering algorithm is obtained by incorporating the feed-forward ALINEA, given by the control law (15a)-(15b). In instances where a traffic incident occurs downstream of on-ramp i, the ramp metering rate is adjusted accordingly as follows:

$$\tilde{r}_i^{\mathsf{coor}}\,(t) = \begin{cases} \max\{\min\{r_i^{\mathsf{loc}}(t), r_i\,(t), r_i^{\mathsf{co}}(t)\}, r_i^{\mathsf{qc}}(t), r_i^{\mathsf{qo}}(t)\} & \text{if } i \text{ is coordinated,} \\ \max\{\min\{r_i^{\mathsf{loc}}(t), r_i\,(t)\}, r_i^{\mathsf{qc}}(t), r_i^{\mathsf{qo}}(t)\} & \text{if } i \text{ is not coordinated.} \end{cases} \tag{18}$$

3 Results and discussion

In this section, we first describe the setup of our case study and then provide a traffic performance evaluation in terms of i) travel time per vehicle, and ii) speed distribution maps.

Experiment setup

For the case study, we consider a 9.1-mile stretch of Interstate 210 Eastbound (I-210 E), which typically comprises four general-purpose traffic lanes and includes 13 on-ramps and 12 off-ramps. Figure 4 illustrates the simulated network in SUMO.

The PM peak period (2:00 PM-7:00 PM), was selected as the study period to evaluate ramp metering strategies, during both peak shoulder and peak hours. Following the FHWA's simulation guidance (Wunderlich et al., 2019), we calibrated the microsimulation model using a representative day approach by utilizing traffic flow and speed data from August 12, 2019. This day has a representative congestion pattern given two incidents, one occurring from 17:10 to 17:50 and the other one from 17:40 to 18:30. The simultaneous perturbation stochastic approximation (SPSA) method (Lee & Ozbay, 2009), due to its efficient approximation of the gradient of the objective function, was applied to calibrate critical parameters (e.g., minimum gap, reaction time, headway

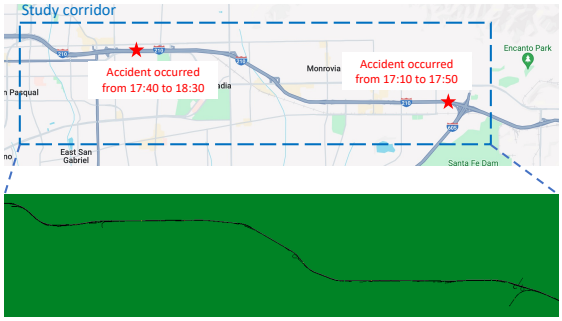

Figure 4: Study corridor of Interstate 210 and locations of traffic accidents.

and lane-changing parameters) automatically to minimize the discrepancy between the simulated and observed performance measure estimates; see Figure 5. The automatic calibration process achieved an acceptable accuracy for the four local and system criteria (Wunderlich et al., 2019) (i.e., time-variant inliers/outliers and bounded dynamic absolute and systematic error) for traffic flow and speed.

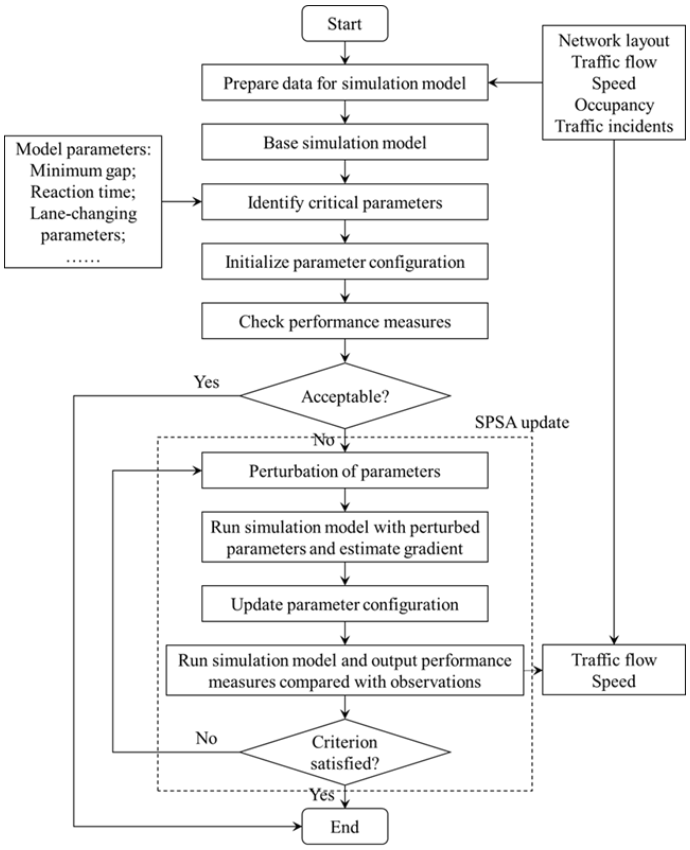

Figure 5: Flowchart of the simulation calibration process.

We defined alternate scenarios by varying CV market penetration, CV roadside infrastructure deployment rates, equipment failure rates, and communication error rates. The settings of each scenario are listed in Table 1. Besides these three scenarios, we consider two benchmarks where the ALINEA and HERO are utilized, respectively.

Comparison of travel time per vehicle

Travel time per vehicle is obtained from dividing total travel time spent, including on-ramp waiting time by all vehicles finishing trips during the time window. Tables 2 and 3 present the results in different scenarios. For local ramp metering, the results indicate that the enhanced algorithm leads

Table 1: Scenarios of CV environment settings.

Parameters	Scenario 1	Scenario 2	Scenario 3
CV Market Penetration Rates	20%	50%	75%
CV Infrastructure Deployment levels	20% of ramps	50% of ramps	80% of ramps
Communication Error Rates	10%	30%	30%
Equipment Failure Rates	15%	9%	3%

to shorter average travel times from 17:30 to 19:00 for Scenario 2 and Scenario 3, with an average reduction of 2.5% in Scenario 2 and of 3.5% in Scenario 3 compared to the baseline scenario. As for system-wide ramp metering, the results show a reduction in average travel time per vehicle in Scenario 1, 2, and 3 of 1.3%, 2.3%, and 6.3% respectively, compared to the baseline scenario.

Table 2: Changes in average travel time per vehicle (in seconds) under locally responsive ramp metering.

	Benchmark	Scenario 1	Scenario 2	Scenario 3
17:15-17:30	990	994 (+0.4%)	991 (+0.1%)	993 (+0.3%)
17:30-17:45	1024	1044 (+2.0%)	990 (-3.3%)	980 (-4.3%)
17:45-18:00	1085	1113 (+2.6%)	1091 (+0.6%)	1058 (-2.5%)
18:00-18:15	1326	1320 (-0.5%)	1284 (-3.2%)	1263 (-4.8%)
18:15-18:30	1334	1345 (+0.8%)	1305 (-2.2%)	1279 (-4.1%)
18:30-18:45	1186	1197 (+0.9%)	1148 (-3.2%)	1137 (-4.1%)
18:45-19:00	810	771 (-4.8%)	754 (-6.9%)	772 (-4.7%)
Avg. reduction		+0.4%	-2.5%	-3.5%

Table 3: Changes in average travel time per vehicle (in seconds) under system-wide ramp metering.

	Benchmark	Scenario 1	Scenario 2	Scenario 3
17:15-17:30	990	993 (+0.3%)	976 (-1.4%)	976 (-1.4%)
17:30-17:45	1012	983 (-2.9%)	983 (-2.9%)	938 (-7.3%)
17:45-18:00	1086	1057 (-2.7%)	1057 (-2.7%)	1016 (-6.4%)
18:00-18:15	1298	1286 (-0.9%)	1283 (-1.2%)	1229 (-5.3%)
18:15-18:30	1282	1262 (-1.6%)	1257 (-2.0%)	1128 (-12.1%)
18:30-18:45	1183	1229 (+3.9%)	1160 (-1.9%)	1182 (-0.1%)
18:45-19:00	743	687 (-7.5%)	700 (-5.8%)	643 (-13.5%)
Avg. reduction		-1.3%	-2.3%	-6.3%

Comparison of speed distribution maps.

Figures 6 and 7 illustrate spatial-temporal freeway mainline speed. As we can see in Figure 6, the CV data-aided locally responsive ramp metering slightly reduced the severity of the congestion between milepost 36 and 38 in Scenario 3 and the tail of the congestion between milepost 31 and 34 in both Scenario 2 and Scenario 3. However, the changes in the length and severity of bottleneck are marginal in Scenario 1. The enhanced system-wide ramp metering further reduced the severity of congestion between milepost 36 and 38 and that between milepost 31 and 34 in both Scenario 2 and Scenario 3. However, similarly to the results from the enhanced locally responsive ramp metering, there is little change in the length and severity of the bottleneck in Scenario 1.

4 Conclusions

In this paper, we proposed using CV data to extract information of distant bottlenecks, induced by traffic accidents, and refining ramp metering algorithms for those bottlenecks. Our method, validated through traffic simulations with emulated BSMs mimicking real-world CV message exchanges, demonstrated that CV data-aided local and system-wide ramp metering algorithms can improve freeway mobility under various conditions, including varying CV market penetration and

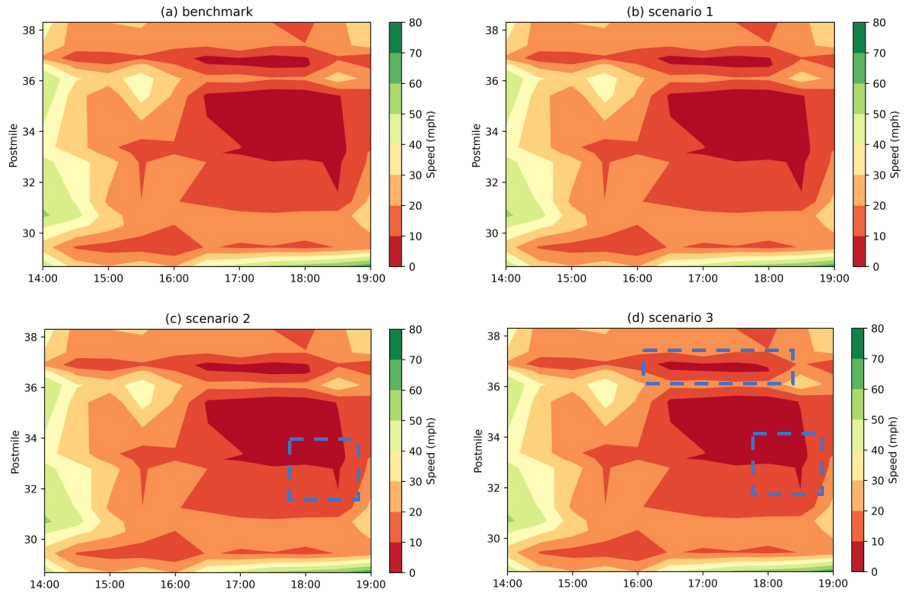

Figure 6: Speed distribution maps under locally responsive ramp metering.

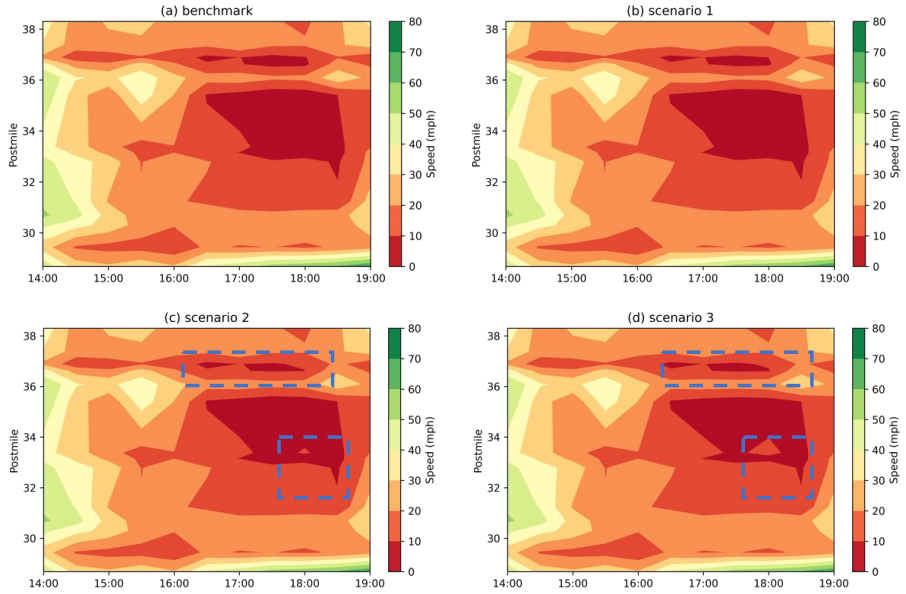

Figure 7: Speed distribution maps under system-wide ramp metering.

infrastructure deployment levels. These findings highlight the potential for improving freeway systems in a CV-enabled environment. It should be noted that the proposed estimation methods are still in an open-loop manner and it is worth investigating control-theoretical approaches to design robust observers for acquiring bottleneck states.

Acknowledgements

The research was performed under the U.S. National Academies of Sciences, Engineering, and Medicine's National Cooperative Highway Research Program (NCHRP) Project 08-145 by Noblis and C2SMART University Transportation Center at New York University. The contents of this paper reflect the views of the authors, who are responsible for the facts and the accuracy of the information presented herein.

References

Frejo, J. R. D., & De Schutter, B. (2018). Feed-forward alinea: A ramp metering control algorithm for nearby and distant bottlenecks. *IEEE Transactions on Intelligent Transportation Systems*, *20*(7), 2448–2458.

Heshami, S., & Kattan, L. (2021). Ramp metering control under stochastic capacity in a connected environment: A dynamic bargaining game theory approach. *Transportation Research Part C: Emerging Technologies*, *130*, 103282.

Hou, Y., Zhang, X., Graf, P., Tripp, C., & Biagioni, D. (2021). A cyber-physical system for freeway ramp meter signal control using deep reinforcement learning in a connected environment. In *2021 ieee international intelligent transportation systems conference (itsc)* (pp. 3813–3820).

Lee, J.-B., & Ozbay, K. (2009). New calibration methodology for microscopic traffic simulation using enhanced simultaneous perturbation stochastic approximation approach. *Transportation Research Record*, *2124*(1), 233–240.

Papageorgiou, M., Hadj-Salem, H., Blosseville, J.-M., et al. (1991). Alinea: A local feedback control law for on-ramp metering. *Transportation research record*, *1320*(1), 58–67.

Papamichail, I., & Papageorgiou, M. (2008). Traffic-responsive linked ramp-metering control. *IEEE Transactions on Intelligent Transportation Systems*, *9*(1), 111–121.

Papamichail, I., Papageorgiou, M., Vong, V., & Gaffney, J. (2010). Heuristic ramp-metering coordination strategy implemented at monash freeway, australia. *Transportation Research Record*, *2178*(1), 10–20.

Smaragdis, E., & Papageorgiou, M. (2003). Series of new local ramp metering strategies. *Transportation Research Record*, *1856*(1), 74–86.

Tajdari, F., Roncoli, C., & Papageorgiou, M. (2020). Feedback-based ramp metering and lane-changing control with connected and automated vehicles. *IEEE Transactions on Intelligent Transportation Systems*, *23*(2), 939–951.

Vasudevan, M., O'Hara, J., Samach, M., Silverstein, C., Asare, S., Townsend, H., ... Zuo, F. (2024). *Utilizing cooperative automated transportation (cat) data for freeway operational strategies* (No. NCHRP Project 08-145).

Vasudevan, M., O'Hara, J., Townsend, H., Asare, S., Muhammad, S., Ozbay, K., ... Zuo, F. (2022). *Algorithms to convert basic safety messages into traffic measures* (No. NCHRP Project 03-137).

Wang, Y., Zhao, M., Yu, X., Hu, Y., Zheng, P., Hua, W., ... Guo, J. (2022). Real-time joint traffic state and model parameter estimation on freeways with fixed sensors and connected vehicles: State-of-the-art overview, methods, and case studies. *Transportation Research Part C: Emerging Technologies*, *134*, 103444.

Wunderlich, K. E., Vasudevan, M., Wang, P., et al. (2019). *Tat volume iii: guidelines for applying traffic microsimulation modeling software 2019 update to the 2004 version* (Tech. Rep.). United States. Federal Highway Administration.

Zhao, Z., Wang, Z., Wu, G., Ye, F., & Barth, M. J. (2019). The state-of-the-art of coordinated ramp control with mixed traffic conditions. In *2019 ieee intelligent transportation systems conference (itsc)* (pp. 1741–1748).

Zhou, Y., Ozbay, K., Kachroo, P., & Zuo, F. (2020). Ramp metering for a distant downstream bottleneck using reinforcement learning with value function approximation. *Journal of Advanced Transportation*, *2020*, 1–13.